sustainability

MDPI

Article

Foundry Sand Waste and Residual Aggregate Evaluated as Pozzolans for Concrete

Guilliana Agudelo [1,2], Carlos A. Palacio [2], Sergio Neves Monteiro [3] and Henry A. Colorado [1,*]

[1] CCComposites Laboratory, Universidad de Antioquia UdeA, Calle 70 No. 52-21, Medellín 050010, Colombia; guiagu1103@gmail.com
[2] Conasfaltos S. A., Medellín 051051, Colombia; capalacio@gmail.com
[3] Departamento de Ciência dos Materiais, Instituto Militar de Engenharia, Rio de Janeiro 22290-270, Brazil; snevesmonteiro@gmail.com
* Correspondence: henry.colorado@udea.edu.co

Abstract: This research is about the utilization of two solid wastes in concrete: foundry sand from the steel smelting process and residual aggregate powder from the asphalt mix production. The solid wastes were added to concrete in contents of 0.0, 5.0, 10, 15, and 20 wt% with respect to cement, and tested in concrete with a design resistance of 280 kgf/cm^2 (27.5 MPa). The effects of these wastes in concrete were compared with commercially available metakaolin, a typical admixture added to concrete, in contents of 0.0, 5.0, 10, 15, and 20 wt% replacing cement content. For all samples, the resistant activity index was evaluated at 28 days. Slump test, air content, density, and compressive strength tests were conducted. The materials' microstructures were evaluated with SEM and XRD after 270 days, in samples immersed in water. Results show that both by-products have pozzolanic activity, classified as N-type pozzolans. Besides, concrete with the residual aggregate powder gave a strength of 541 kgf/cm^2 (53.1 MPa), which corresponds to sample M4 (concrete containing 15% residual aggregate powder), consistent with 93% improvement with respect to the strength resistance. Furthermore, concrete with the foundry sand powder gave a strength of 561 kgf/cm^2 (55 MPa), consistent with 100% improvement with respect to the strength resistance, which corresponds to M15 (concrete containing 20% foundry sand). Concrete with the metakaolin powder presented a strength of 609 kgf/cm^2 (59.7 MPa), which corresponds to M9 (concrete containing 15% metakaolin), consistent with 116% improvement with respect to the strength resistance. The concrete developed with the by-products can be produced at lower costs than traditional admixtures, which guarantees the feasibility of the environmental solution.

Keywords: concrete; solid wastes; compressive strength; foundry sand; residual aggregate; metakaolin; pozzolanic activity; lower costs

Citation: Agudelo, G.; Palacio, C.A.; Neves Monteiro, S.; Colorado, H.A. Foundry Sand Waste and Residual Aggregate Evaluated as Pozzolans for Concrete. *Sustainability* **2022**, *14*, 9055. https://doi.org/10.3390/su14159055

Academic Editor: José Ignacio Alvarez

Received: 26 May 2022
Accepted: 7 July 2022
Published: 24 July 2022

1. Introduction

There is an increasing need for producing environmentally and economically sustainable solutions not only from governments but also from society, even more because structural materials are by weight one of the biggest contributors to greenhouse gases and freshwater consumption. Of course, there are positive aspects as well: construction and building materials can hold a high content of liquid and solid wastes, particularly concrete [1], asphalt pavement [2], geopolymers [3], phosphates [4], and soil [5–7].

In some countries, there is still no specific use for some solid wastes, which is why managing to incorporate these wastes into construction materials is a great advance in achieving adequate sustainable waste management [8].

In Colombia, companies are being forced to go green with multiple regulations and tax exemptions. Conasfaltos is a large infrastructure company producing around four tons/day of residual aggregate powder, currently disposed of in a landfill, and now being one of the leaders in the sector in transitioning to a circular economy. On the other hand, there are

foundry companies that produce about one ton/day of sand waste, used for iron smelting. In addition, Colombia has very important mines of kaolin, producing large amounts of metakaolin, which is widely used in the construction industry in many applications, such as supplementary cementitious material. This is because metakaolin has greater pozzolanic activity due to its highly reactive amorphous phase, which occurs after the calcination of kaolinite [9–12].

Pozzolans usually react with portlandite to form more stable compounds, which can limit the amount of calcium and alkalis [13]. The higher the pozzolan content, the lower the final portlandite concentration. Special care must be taken when dosing pozzolans such as ashes since high doses can produce other durability issues [14], although it has been found that with the use of pozzolans, concrete can have greater durability [15,16]. These pozzolans have also been studied via artificial networks in alternative materials such as geopolymers [17]. Some authors have used concrete demolition and the recycling of rubble in combination with additions of natural pozzolans to mitigate environmental side effects [18]. Volcanic pozzolans and rice husk have also been studied due to their high silica contents [19,20], whereas lamp glass waste has been used to evaluate reactivity by replacing fine aggregates instead of cement [21,22]. The classification of pozzolans according to Colombian Technical Standard 3493 is as follows: Class N: natural, calcined, or raw pozzolans such as some diatomaceous soils, flint and opaque shales, tuffs and volcanic ash, or pumice stone [23]. Class F: fly ash produced in the burning of anthracitic or bituminous coal. This class of fly ash has pozzolanic properties [23]. Class C: fly ash produced from lignite or sub-bituminous coal, which having pozzolanic properties, possesses cementing properties. Some class C ashes have lime contents greater than 10% [23].

On the other hand, foundry sand is a high-quality silica sand, a solid waste by-product of the smelting production of ferrous and non-ferrous metals, therefore typically containing several hazardous metals. Raw sand (base sand) is usually of higher quality than natural sand used in construction. Foundry sand consists of 85–95% high-quality silica sand, 7–10% bentonite or kaolinite clay, 2–5% water, and approximately 5% charcoal [24–26]. In the smelting process, the molding sand is recycled and reused several times and is degraded to the point where the old sand is removed from the cycle as a by-product, new sand is introduced, and the cycle starts over. The smelting of foundry sand results in large volumes that cannot be stored. Since foundry sand is basically a fine aggregate, it can be used in many ways [27].

In Colombia, the aggregates that are used in the production of hydraulic concrete are exploited mainly in mountainous areas. As these sites have difficult geography, heavy machinery must be used, which generates more expenses but is also a source of employment for local people [28].

Differently, metakaolin (MK) [29] is a thermally activated alumina–silicate, obtained by calcining kaolin clay in a temperature range of 650 to 800 °C. Due to its high pozzolanic properties, the use of MK as an addition to concrete has attracted high interest in recent years. An important difference between MK and other supplementary cementitious materials is that MK is a primary product, whereas others are by-products. Therefore, MK can be produced in a controlled process to achieve desired properties. The use of MK improves the compressive strength of concrete, especially during the first stages of hydration. The increase in concrete strength with MK is because MK particles fill the space between cement particles and accelerate cement hydration and pozzolanic reaction. However, after 14 days, the contribution that MK makes to the strength of concrete is reduced [29]. The concrete consumption is quite large elsewhere. It has been estimated that cement consumption worldwide was approximately 3309 million metric tons in 2018 [30,31]. In Colombia, from January to May of 2019, ready-mix concrete production reached a volume of 2.83 million cubic meters [32]. Thus, with the use of the solid wastes selected in this research, the impact on cement consumption can be very significant. There are several research gaps in the use of these wastes, the main one being the combination of them now with the

shortage of raw materials and useful wastes for concrete. This research aims to make these solutions sustainable not only ecologically but economically as well. Additionally, few of the studies have real applications and are mostly at a laboratory scale, and do not involve large companies in the construction sector.

The main goal of this investigation is to develop mixtures of hydraulic concrete with MK and two local industrial by-products: residual aggregate powder and sand waste from the iron smelting process. Thus, the novelty is a project with a potential technical collaborative solution for several large industries: aggregates, steel making, and concrete industry. This collaborative solution is required for the industrial parks in Colombia, where companies can reduce important logistics costs with smart cooperation. Moreover, this research is applied in the large industry of Medellín, Colombia. Another important objective is to evaluate whether the by-products can be used as natural pozzolans as defined by the ASTM. It is expected that the mechanical performance and durability of concrete with these wastes can be similar or competitive to concrete with MK. The circular economy of materials [33–35] and processes [36–38] is very important today, and this research contributes not only to reducing pollution but also to showing other similar industries how to make an impact on these topics.

2. Experiments

Aggregates used in concrete mix designs were provided by the company Conasfaltos SAS from materials produced in Colombia. Coarse and 3/4" aggregates were used in concrete. The coarse sand used was obtained by classifying river material in Medellín; its gradation is shown in Figure 1a. Figure 1b shows gradation of 3/4" (19 mm) aggregate, obtained through primary crushing and classification processes. Table 1 shows the physical properties of these aggregates. The cement used was type III structural cement, typically used for high early strengths; its properties are summarized in Table 2.

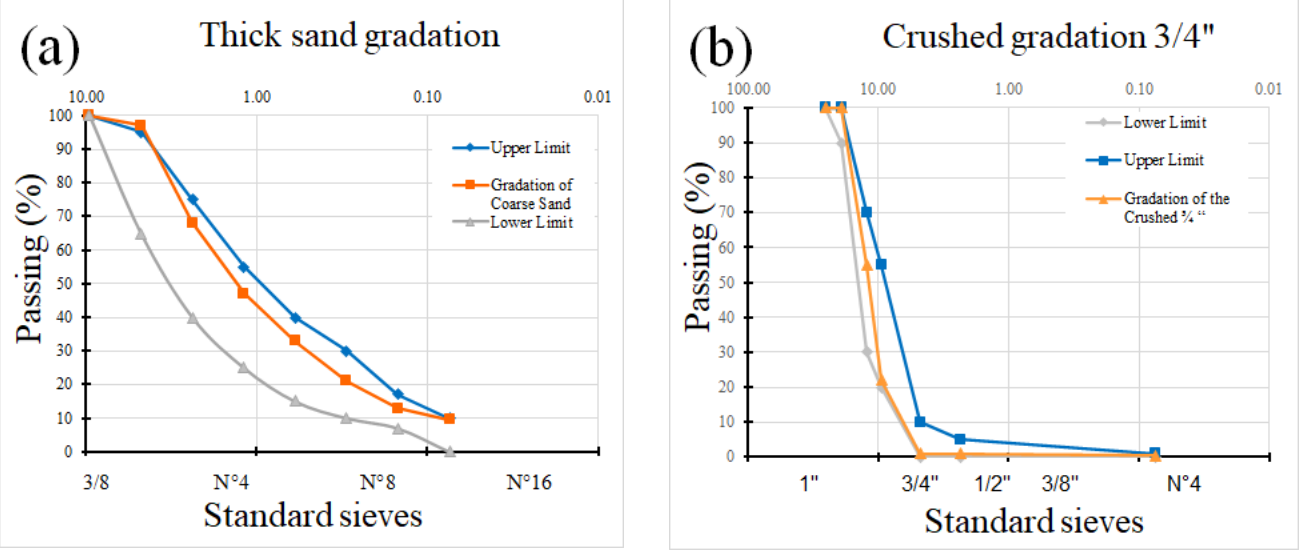

Figure 1. Gradation of river material in Medellín (**a**) sand and (**b**) crushed 3/4".

The metakaolin (MK) was used as additive reference material in order to establish comparisons with the by-product's performance in concrete; see its properties in Table 3. Two types of materials were used as additives: residual aggregate powder (a by-product of asphalt mix production) and foundry sand. These two materials were evaluated as natural pozzolans. Table 3 shows the characterization of the foundry sand and the by-product (residual aggregate powder-PB).

Table 1. Specifications of used aggregates.

Test	Unity	Gross Sand	Fine Specification	Crushed 3/4″	Thickness Specification	Ref.
Clay lumps	%	1.7	3 (Max)	1.9	3 (Max)	[39]
Unitary loose mass	(Kg/m^3)	1652	-	1414	-	[40]
Empty	%	38.4	-	46.5	-	
Compact unit mass	(Kg/m^3)	1787	-	1506	-	[40]
Apparent specific weight		2.637	-	2.604	-	[41]
Apparent specific weight (s.s.s.)		2.686	-	2.660	-	[41]
Nominal specific weight		2.783	-	2.759	-	[41]
Absorption	%	2.10	-	2.15	-	[41]
Wear 500 revolutions	%	N/A	N/A	23.9	40 (Max)	[42]
Particles with a fractured face	%	N/A	N/A	100	60 (Max)	[42]

Table 2. Cement properties.

Test	Result	Specification	Ref.
Specific Surface Blaine (m^2/kg)	363	280	[43]
(%) retained Sieve 325	5.3		[44]
Change of length by Autoclave (%)	0.17	0.8 Max.	[45]
Initial setting time (min)	108	45 min Min	[46]
Final setting time (min)	203	450 min Max	[46]
Air content in mortar (%)	5.3		[47]
Compression resistance to 1 day (MPa)	17.3	-	[48]
Resistance to compression to 3 days (MPa)	30.1	10 MPa Min	[48]
Compressive strength at 7 days (MPa)	34.7	19.5 MPa	[48]
Compressive strength at 28 days (MPa)	40.6	28 MPa	[48]
Mortar bar expansion to 14 days (%)	0.01		[49]

Table 3. Properties of foundry, metakaolin sand, and residual aggregate powder-PB.

Test	Result Foundry Sand	Result Residual Aggregate Powder	Result Metakaolin	Specification	Ref.
Apparent Density	2.04 kg/m^3	2.663 kg/m^3	0.35–0.45 kg/m^3	N.A	[23,50]
Humidity percentage	4.7%	4%	<3%	3% Max.	[23,50]
Lost to fire	17%	11%		10% Max	[23,50]
Fineness	65.4%	69.5		34 Min	[23,50]
Resistant activity index 28 days	75.4%	77.7%	87%	75% min	[23,50]
Color	Black	Light brown	Gray–light gray	-	[23,50]
Lost by ignition, PPI at 800 °C	-	-	<2.5%	<10%	
SiO_2	65.93%			70% Min	[23,50]
Aluminum oxide	14.78%				[23,50]
Iron oxide	6.03%				[23,50]

Table 3. *Cont.*

Test	Result Foundry Sand	Result Residual Aggregate Powder	Result Metakaolin	Specification	Ref.
Magnesium oxide	6.45%				
Sulfur trioxide	0.14%			4% Max	[23,50]
Potassium oxide	0.543%				
Titanium dioxide	0.242%				
Phosphorus pentoxide	0.090%				
Zinc oxide	1.147%				
$Ca_2(Mg,Fe,Al)_5(Al,Si)_8O_{22}(OH)_2$	-	24.1%			
SiO_2.FeO. CaO	-	18.1%		70% Min	
$Al_2O_3.2SiO_2.2H_2O$	-	6.1%			
$SiO_2.Al_2O_3.Fe_2O_3$	-	31.9%	>85%		[23,50]
SiO_2	-	14%		>70%	
$Na_2O{\cdot}Al_2O_3{\cdot}6SiO_2$	-	5.8%			
SO_3	-	-	<5%	<40%	

A plasticizer admixture that complies with type A and F standards [51], for chloride-free or other materials with oxidation potential, was used to give manageability for approximately half an hour and for reducing the amount of water in the designs. Slumps of 18 cm were sought because this concrete can be pumped; the dosage was 0.7% of the weight of the cement.

The experimental design followed in this research was the categorical factor, obtained in STATGRAPHICS (see Table 4). This method was considered because three variables were used as additives (metakaolin, residual aggregate powder-PB, and foundry sand); but the variables are independent and no combinations between them were evaluated.

Table 4. Experimental design.

Sample	Equivalence in Statgraphics	% Addition	Type of Addition
M1=M6=M11	1	0%	-
M2	2	5%	residual aggregate powder
M3	3	10%	residual aggregate powder
M4	4	15%	residual aggregate powder
M5	5	20%	residual aggregate powder
M1=M6=M11	1	0%	-
M7	2	5%	metakaolin
M8	3	10%	metakaolin
M9	4	15%	metakaolin
M10	5	20%	metakaolin
M1=M6=M11	1	0%	-
M12	2	5%	foundry sand
M13	3	10%	foundry sand
M14	4	15%	foundry sand
M15	5	20%	foundry sand

Concrete mixtures were made by evaluating each variable in a wide range of percentages, from 0 to 20 wt% of the cement. In this design, each factor or variable is independent and takes equally spaced values, usually taken as 1, 2, 3, 4, and 5; which are equivalent to percentages of each variable between 0, 5, 10, 15, and 20%. For the experiments described in this investigation, the three main variables were: industrial by-product 1 (residual aggregate powder-PB), industrial by-product 2 (foundry sand), and MK. The time during which the evolution of the resistance of each sample was measured was from 3 to 270 days. The additions of by-products and MK were then evaluated in concrete with a strength of 280 kgf/cm^2 (27.5 MPa), one of the most commercially used and therefore representative of the construction sector.

The design method followed in this research is based on the Vitervo O'Reilly Díaz method [52], which takes the following steps: determination of the required strength, the maximum size of the coarse aggregate, maximum size of the sand and the fineness modulus ranges, slump determination, calculation of the water/cement ratio, the amount of cement per cubic meter, and the determination of the optimal ratio of coarse and fine aggregates. Table 5 shows the concrete designs with residual aggregate powder-PB. Table 6 shows the designs evaluated with MK. Table 7 shows the designs made with foundry sand.

Table 5. Concrete design with residual aggregate.

Sample	Resistance, kg/cm^2 (MPa)	Cement (kg)	Residual Aggregate Powder (kg)	Water (kg)	Water/Cement Ratio (Ad)	Sand (kg)	Gravel (kg)	Sand/Gravel (%)	Additive (kg)
1	280 (27.5)	350	0	180	0.514	1009	826	55/45	2.45
2	280 (27.5)	350	17.5	180	0.490	1009	826	55/45	2.45
3	280 (27.5)	350	35	180	0.468	1009	826	55/45	2.45
4	280 (27.5)	350	52.5	180	0.447	1009	826	55/45	2.45
5	280 (27.5)	350	70	180	0.429	1009	826	55/45	2.45

Table 6. Concrete design with metakaolin.

Sample	Resistance, kg/cm^2 (MPa)	Cement (kg)	Metakaolin (kg)	Water (kg)	Water/Cement Ratio (Ad)	Sand (kg)	Gravel (kg)	Sand/Gravel (%)	Additive (kg)
6	280 (27.5)	350	0	180	0.514	1009	826	55/45	2.45
7	280 (27.5)	350	17.5	186	0.506	1000	818	55/45	2.45
8	280 (27.5)	350	35	187	0.486	999	817	55/45	2.45
9	280 (27.5)	350	52.5	200	0.497	975	798	55/45	2.45
10	280 (27.5)	350	70	215	0.512	949	776	55/45	2.45

Table 7. Concrete design with foundry sand.

Sample	Resistance, kg/cm^2 (MPa)	Cement (kg)	Foundry Sand (kg)	Water (kg)	Water/Cement Ratio (Ad)	Sand (kg)	Gravel (kg)	Sand/Gravel (%)	Additive (kg)
11	280 (27.5)	350	0	180	0.514	1009	826	55/45	2.45
12	280 (27.5)	350	17.5	196	0.559	986	807	55/45	2.45
13	280 (27.5)	350	35	196	0.559	986	807	55/45	2.45
14	280 (27.5)	350	52.5	196	0.559	986	807	55/45	2.45
15	280 (27.5)	350	70	196	0.559	986	807	55/45	2.45

In total 21 cylindrical samples of 10 × 20 cm^2 each were made for each concrete formulation (numbered M1 to M15), for a total of 315 concrete cylinders. For each percentage of the addition, three cylinders were tested for each age. The ages of the tests were: 3, 14, 28, 56, 90, 180, and 270 days. All cylindrical samples were kept submerged in water during the tested period. The air content for each sample and the density were measured. The

compressive strength of all samples was measured in a Controls CT-1303 press. Scanning electron microscope (SEM) characterization was performed with an energy dispersive spectroscopy (SEM–EDS) type JEOL JSM-6490LV operated in a high vacuum mode, used to observe the microstructure and chemical composition of the samples. Petrography tests were also included.

The cost of the concrete was determined based on the internal production costs for the company. The cost of MK and the cost of production of the by-products were taken from the Colombian market.

3. Results and Analysis

Petrography on the aggregates for gravel fractions below $\frac{1}{2}$" showed the following results: volcanic andesite (40.2%), amphibolite (21.4%), quartzite (15.2%), andesite (3.5%), microgram (7.8%), silicate andesite (3.5%), chert (1%), alternating volcanic rock (9%), sublioarenite (0.3%), and altered gaps (1.6%). Aggregates tend to be sub-granular with some sphericity. The porosity of the sample was estimated at 3.8%, and the percentages of fractures at the macroscopic and microscopic levels were estimated at 0.3%.

Figure 2a shows the EDS spectrum of the aggregates, with Si, Ca, Mg, and Fe as the main elements forming oxides. Table 8 shows the quantification presented by the evaluated aggregate, where their components were quantified via Rietveld analysis, finding albite (46.1%), clinochlore (23.2%), muscovite (12.8%), quartz (9.9%), and amphibole (7.9%). In the spectrum, the aggregate used has silica and alkalis in its composition, containing sodium and potassium. Results of the SEM are shown in Figure 2b, which has an average size of 3 mm. The discontinuous and rough surface of the aggregate with a non-homogeneous surface can be appreciated. The sample contains silica, aluminum, magnesium, oxygen, calcium, iron, sodium, and potassium.

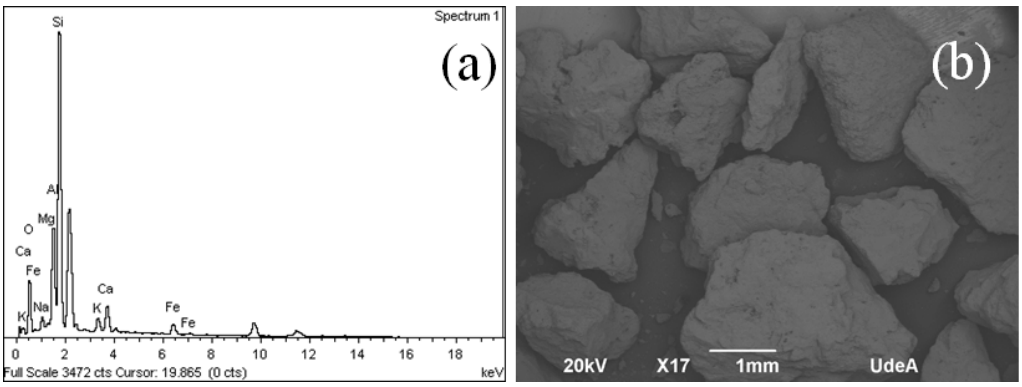

Figure 2. SEM of the aggregate (**a**) under study from the center of Colombia and (**b**) quantification of composition aggregates.

Table 8. Composition quantification of aggregate.

	Compound				
Sample	**% Quartz**	**% Albite**	**% Muscovite**	**% Amphibolite**	**% Clinochlore**
Aggregate	9.9	46.1	12.8	7.9	23.2

Figure 3 shows the XRD for cement, where most representative peaks are analyzed and the cement composition is presented in Table 9: quartz (28%), lime (11%), periclase (7%), tricalcium aluminate (13%), calcite (21%), and goethite (20%). Figure 3 shows the spectrum for MK: quartz (92%) and cristobalite (8%). In Figure 3, the spectrum of residual aggregate powder-PB is presented, and in Table 9, the quantified composition is summarized. This contains minerals such as quartz (13%), oligoclase (23%), hornblende (19%), albite (21%), chamosite (7%), and tremolite (17%). Figure 3 shows the spectrum of the foundry sand,

and in Table 9 the composition is summarized. This contains quartz (55%), brucite (6%), franklinite (2%), protoenstatite (7%), and kyanite (30%).

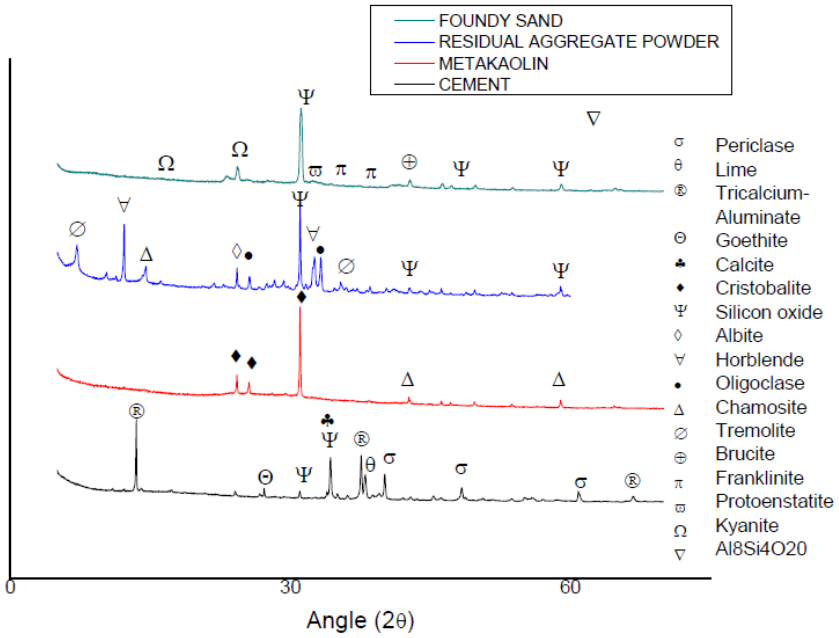

Figure 3. XRD for the raw materials.

Table 9. Concrete design with foundry sand.

Sample	Cement	Metakaolin	Residual Aggregate Powder-PB	Foundry Sand
% Silice Oxide	28	-	13	55
% Lime	11	-	-	-
% Periclase	7	-	-	-
% Tricalcium aluminate	13	-	-	-
% Calcite	21	-	-	-
% Goethite	20	-	-	-
% Cristobalite	-	38	-	-
% Oligoclase	-	-	23	-
% Hornblende	-	-	19	-
% Albite	-	-	21	-
% Chamosite	-	-	7	-
% Tremolite	-	-	17	-
% Brucite	-	-	-	6
% Franklinite	-	-	-	2
% Proto-enstatite	-	-	-	7
% Kyanite	-	-	-	30
% $Al_8Si_4O_{20}$		62		

The SEM characterization for the cement is presented in Figure 4a, showing a large number of particles of different sizes, which indicates the presence of ashes. Figure 4b shows SEM for metakaolin, which is known to be partially crystalline [53], revealing different particle sizes. Figure 4c shows the results of the SEM for the residual aggregate powder, which has a cement-like structure, and clearly is not homogeneous. Figure 4d is

the SEM of the foundry sand, showing more homogeneous particle sizes with an elongated type grain [54].

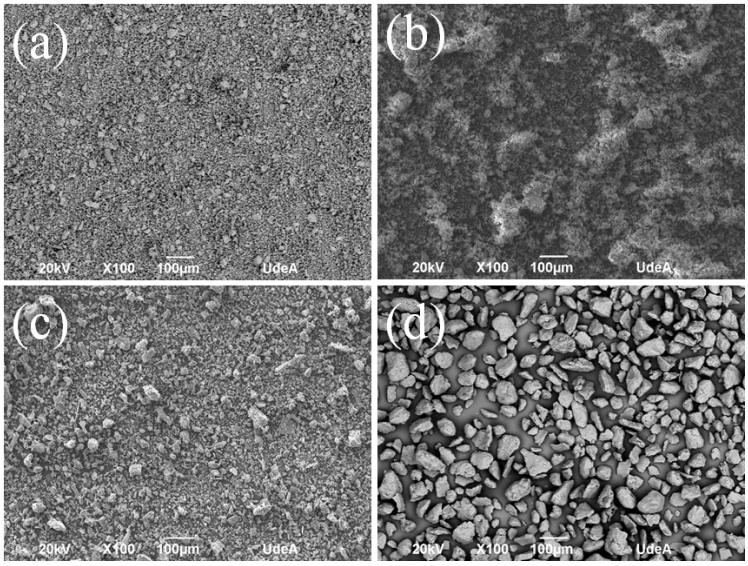

Figure 4. SEM characterization (**a**) cement, (**b**) metakaolin, (**c**) residual aggregate powder, and (**d**) foundry sand.

Table 10 shows the quantification of the elemental composition of each raw material, which reveals that the foundry sand and the residual aggregate powder have a high silica content, even greater than cement, whereas the metakaolin is relatively low.

Table 10. Elemental quantification of the of raw materials.

Sample	**Element**									
Element Content	**% O**	**% Na**	**% Mg**	**% Al**	**% Si**	**% K**	**% Ca**	**% Fe**	**% C**	**% Ti**
Cement	36.35	-	1.22	1.52	7.52	-	41.51	1.97	9.91	-
Metakaolin	42.66	-	-	22.59	29.77	-	-	3.21	-	1.77
Residual aggregate powder-PB	35.05	-	1.31	2.49	42.3	-	0.9	4.83	13.14	-
Foundry Sand	30.63	-	2.11	12.22	39.98	-	1.62	13.55	-	-

All samples were prepared with a constant water to cement (w/c) ratio, but this ratio was a function of each of the additions (residual aggregate powder, foundry sand, or metakaolin). With metakaolin, the w/c ratio increased in the mixtures, because they were not sufficiently hydrated, and adding water was necessary, which did not affect the final strength. It is known that metakaolin tends to dry the mixtures, and that is why a higher w/c ratio is required in order to find the desired consistency [55]. For the two by-products, the w/c ratio remained constant and the addition of water to the design was not necessary. In all the sample formulations (M1 to M15), the air content and the manageability of the concrete were measured, the mixing process was started, and after one hour, the property was evaluated with the settlement test [56]. Samples were broken using a Controls CT-1303 press, following the corresponding standards [57]. The density of each concrete produced was also measured.

Figure 5a–c shows all samples (M1 to M15) tested after 270 days of being submerged, the aggregate is covered homogeneously by the cement paste, and there is no particle detachment at the time of failure. In addition, the concrete mixtures were cohesive. On the other hand, it is evident that the failures were due to the cut type of all samples, some to a greater extent than the others.

Figure 5. Samples tested under compression (**a**) M1 to M5, (**b**) M6 to M10, and (**c**) M11 to M15.

Table 11 shows a summary of the properties evaluated for fresh concrete mixtures which contained the additions of metakaolin, residual aggregate powder-PB, and foundry sand, from M1 to M15 (experimental design). For each concrete mixture, compressive strength was tested after 270 days of being submerged in water. Density was measured on freshly prepared concrete, which is very similar for all the samples (around 2400 kg/m^3). The fresh air content was measured (between 1.2% and 2%); it was sought that the air content did not exceed 3%, since this helps to achieve more durable concrete.

Table 11. Summary of evaluated properties of fresh concrete samples M1–M15.

Sample	Compressive Strength 270 Days (kgf/cm^2)	Density (kg/m^3)	Air Content (%)
M1	349	2436	1.2
M2	349	2433	1.9
M3	434	2435	1.5
M4	541	2436	1.3
M5	440	2405	2
M6	349	2436	1.2
M7	528	2411	1.4
M8	559	2415	1.8
M9	609	2436	1.3
M10	590	2437	1.9
M11	349	2436	1.2
M12	472	2414	1.9
M13	493	2438	2
M14	534	2448	1.6
M15	561	2458	1.4

Figure 6a shows the evolution strength for samples M1 to M5 starting at day 3 up to day 270, produced with the PB residual aggregate powder. Dosages evaluated using the residual aggregate powder as a replacement help achieve the design resistance of 280 kgf/cm^2 (27.5 MPa). With the 15% addition (M4), the highest strength of 541 kgf/cm^2 (53.1 MPa) is reached, whereas with 20% (M5) the strength was 440 kg/cm^2 (43.1 MPa). Figure 6b shows the slumps of the four samples with residual aggregate powder (M2–M5) and the standard sample (M1). This property is measured at the initial time of the test and one hour later for the five samples, measuring the workability of concrete. At the initial time, the five samples showed good manageability (zero hours). The settlements obtained were between 16 and 18 cm. These results are within the expected range for concrete that can be pumped. After an hour, workability was lost, because the slump went from between 16 and 18 cm to between 5 and 8 cm. The error is shown for each of the samples at the ages of failure, which are not pronounced, showing that the values obtained are reliable. Figure 7a,c,e,g,i shows the initial settlements of the samples evaluated with residual aggregate powder, and the appearance of the mixtures right after production is presented. Figure 7b,d,f,h,j shows slumps after an hour, evidencing that the mixtures lost manageability and were not workable.

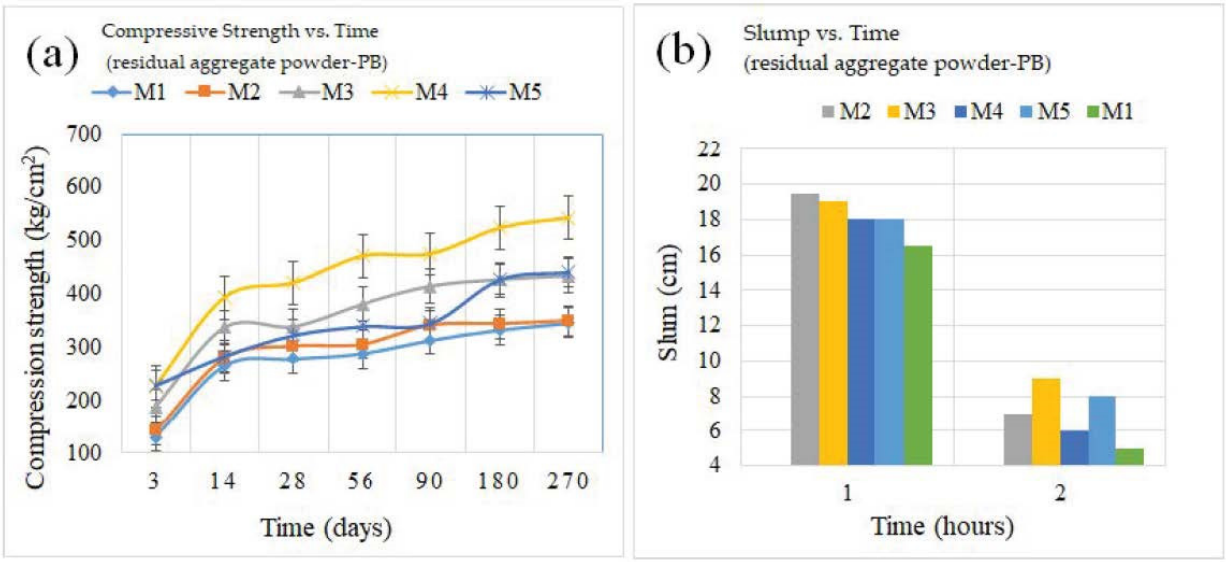

Figure 6. Evolution strength for samples M1 to M5 (**a**) compressive strength development; (**b**) slump.

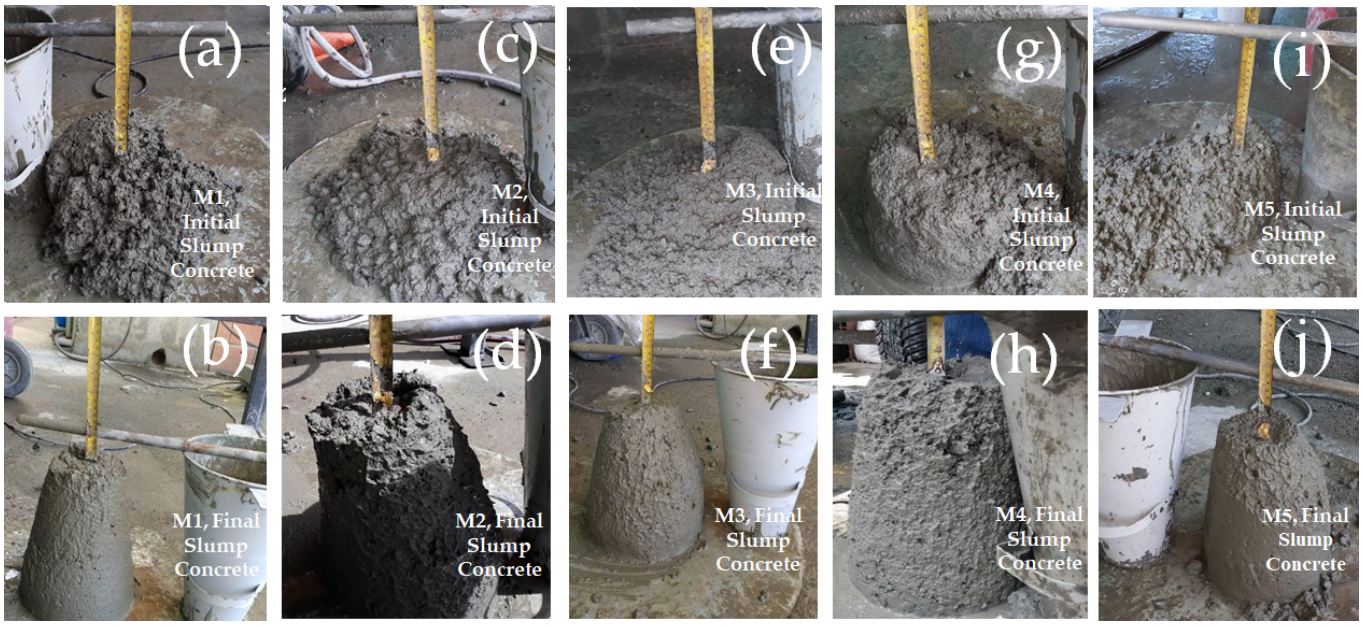

Figure 7. Figure of the slump, standard ASTM C143 of the five mixtures evaluated with residual aggregate powder, shows the initial and final slumps.

Figure 8a shows the strength evolution of samples M6 to M10, produced with metakaolin, starting at day 3 and up to day 270. With 15% of metakaolin (M9), the highest strength of 609 kg/cm^2 (59.7 MPa) was reached, whereas with 20% (M10) strength begins to decrease reaching 590 kg/cm^2 (57.9 MPa). The design strength was achieved in all samples, but the highest peak was obtained with a 15% addition. The increase in concrete strength with the addition of metakaolin was largely due to the formation of an optimal microstructure within the concrete [58]. Figure 8b shows the slumps of all four samples made with metakaolin (M7–M10) and the standard sample (M6). This property was measured at the initial time of the test and one hour later for all samples. All of them showed, at the initial time, good workability, and the slumps were between 16 and 18 cm, all within the expected range. After an hour, the workability was lost, showing results between 6 and 10 cm with acceptable error bars, suggesting a reliable material. Figure 9a,c,e,g,i shows the initial slumps and Figure 9b,d,f,h,j shows the slumps after an hour, clearly losing workability.

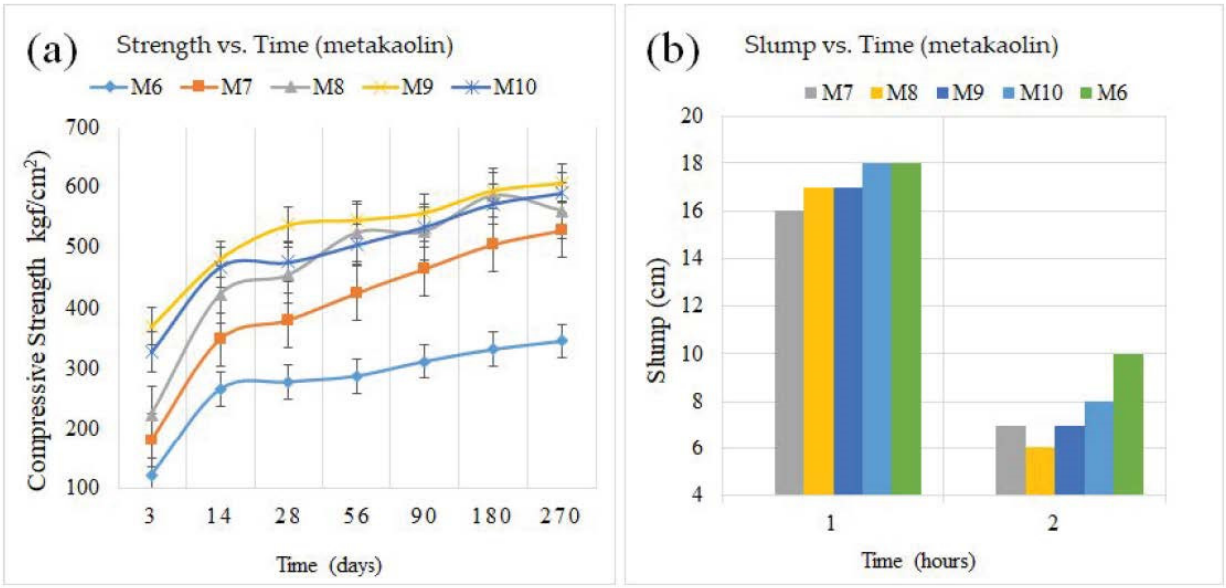

Figure 8. Strength evolution for samples M6 to M10 (**a**) compressive strength development and (**b**) slump.

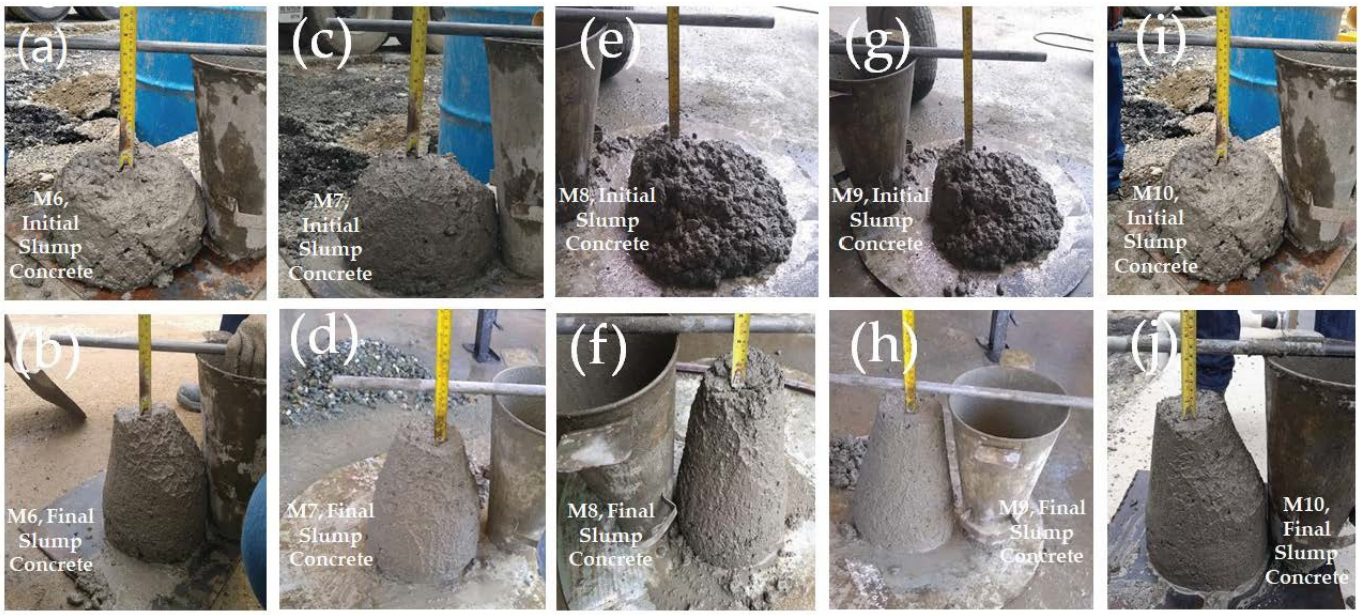

Figure 9. Standard ASTM C143 of the five mixtures evaluated with metakaolin, showing the initial and final slumps.

Figure 10a shows the strength evolution for samples M11 to M15, starting at day 3 and up to day 270, produced with foundry sand. With 20% of the addition (M15), the strength of 561 kgf/cm^2 (55 MPa) was achieved. The design resistance was achieved in all samples, but the highest peak was obtained with a 20% addition of the foundry sand. Figure 10b shows slumps of the four samples made with the foundry sand (M12–M15) and the standard sample (M11). All five samples produced, at the initial time, good workability with slumps between 18 and 20 cm, all within the expected range. After an hour, the workability was lost to values between 6 and 10 cm, and the error bars suggested a very reliable material. Figure 11a,c,e,g,i shows the initial slumps, whereas Figure 11b,d,f,h,j shows slumps after an hour, where there is evidence that the mixtures lost workability.

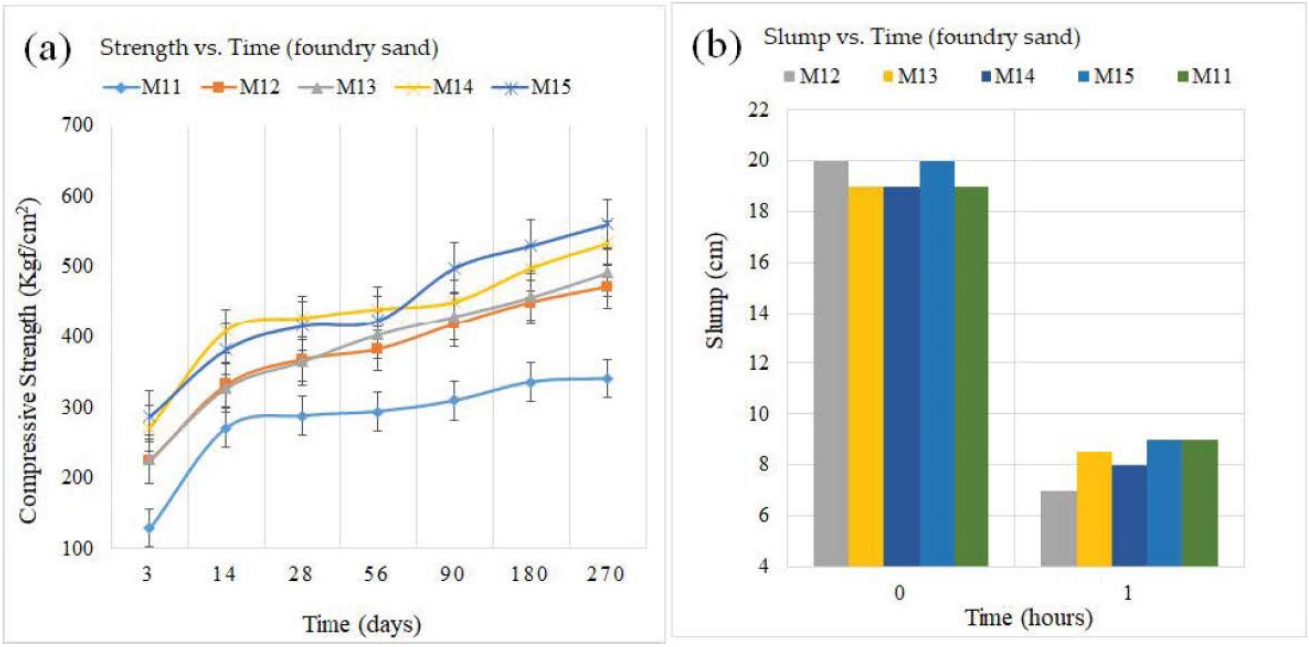

Figure 10. Strength evolution for samples M11 to M15: (**a**) compressive strength development and (**b**) slump.

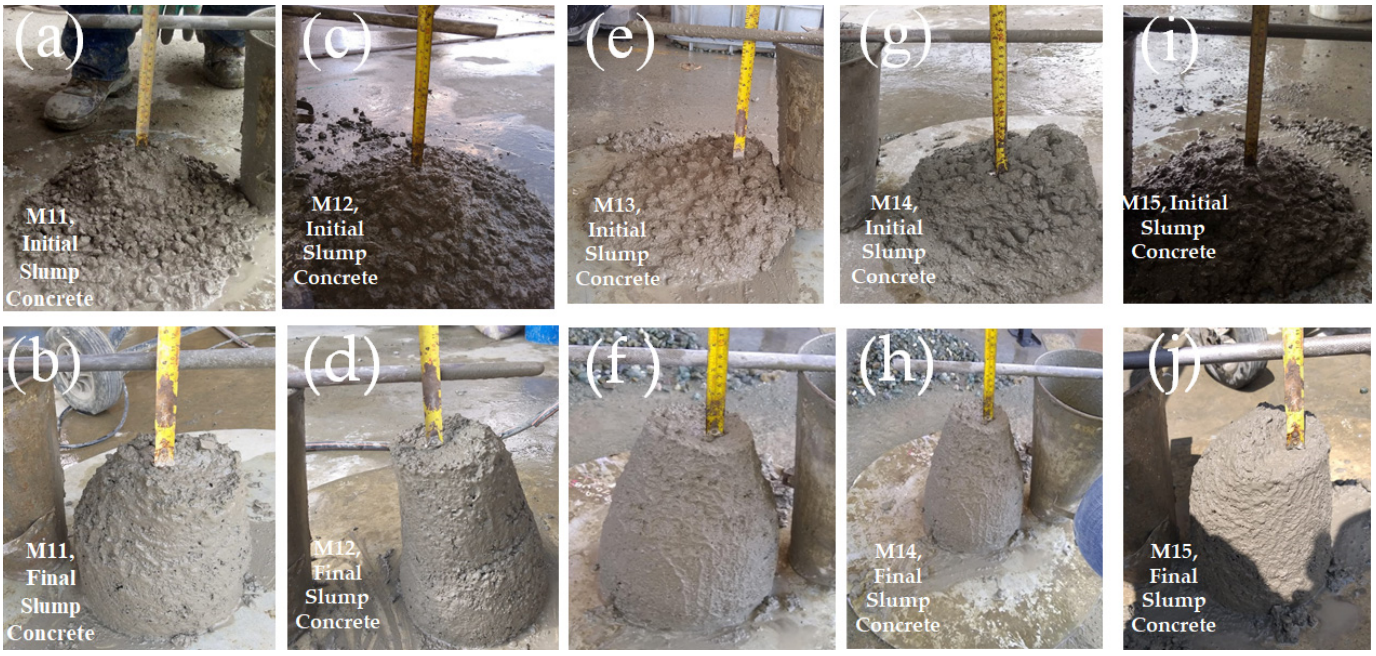

Figure 11. Slumps of the five mixtures evaluated with metakaolin, following the standard ASTM C143, showing the initial and final slumps.

Figure 12 shows the XRD for samples of standard concrete and samples including the residual aggregate powder-PB (M1–M5) after 270 days. Each peak was identified and the quantification of the crystalline phases is summarized in Table 12. All samples have quartz and calcite, and excepting samples M5, also contain cristobalite. Other identified phases are albite and ettringite, hornblende, greenalite, cordierite, oligoclase, portlandite, ferrobustamite, anorthoclase, and annite.

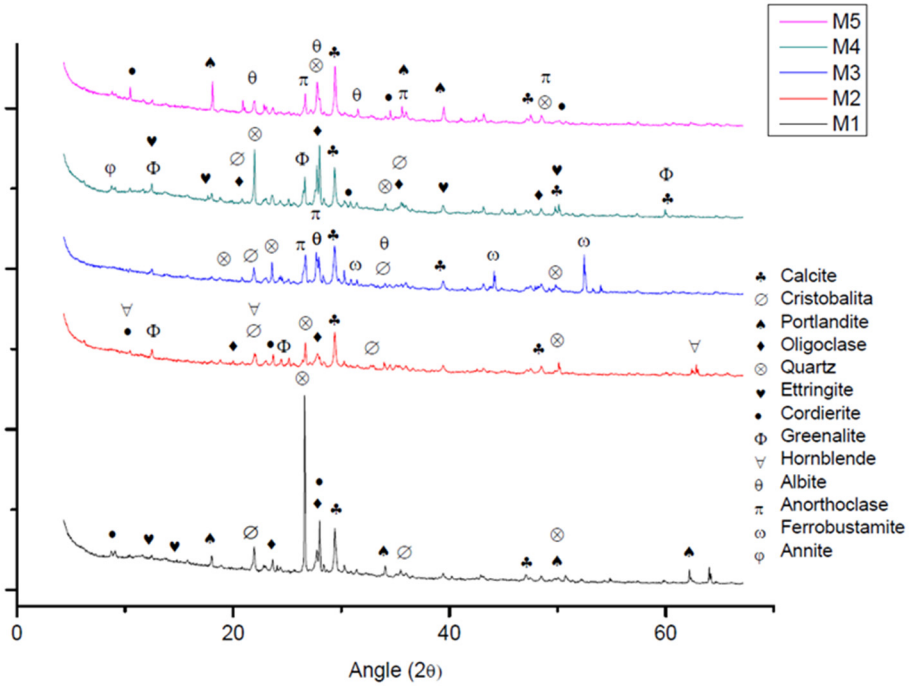

Figure 12. XRD after 270 days M1, M2, M3, M4, and M5.

Table 12. Quantification of composition found by XRD—residual aggregate powder.

	Samples				
Compound	**M1**	**M2**	**M3**	**M4**	**M5**
% Calcite	9.1	19	10.1	8	15.2
% Cristobalite	4	3	3	6	-
% Quartz	46.5	10	6	6	6
% Albite	-	-	37.4	-	33.3
% Ettringite	3	-	-	2	-
% Hornblende	-	13	-	-	-
% Greenalite	-	8	-	3	-
% Cordierite	12.2	13	-	7	15.2
% Oligoclase	23.2	34	-	66	-
% Portlandite	2	-	-	-	3
% Ferrobustamite	-	-	18.2	-	-
% Anorthoclase	-	-	25.3	-	27.3
% Annite	-	-	-	2	-
Total	100	100	100	100	100

Figure 13 shows XRD for samples of standard concrete and samples including metakaolin after 270 days (M6–M10). Each peak was identified, and the quantification of the crystalline phases is summarized in Table 13. All samples contained quartz, calcite, cristobalite, and oligoclase. Other identified phases are albite, ettringite, ferrosilite, enstatite, cordierite, portlandite, chamosite, and anorthoclase.

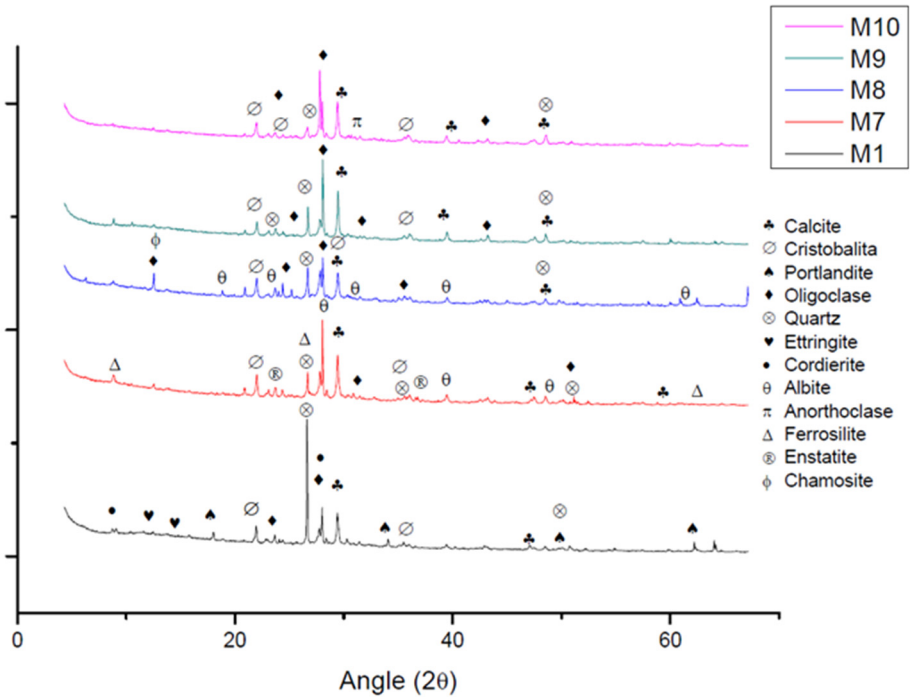

Figure 13. XRD after 270 days M1, M7, M8, M9, and M10.

Figure 14 shows XRD for samples of standard concrete and samples with foundry sand after 270 days (M11–M15). Each peak was identified, and the quantification of the crystalline phases is summarized in Table 14. All samples contained quartz and calcite. Other identified phases are cristobalite, albite, ettringite, cordierite, oligoclase, portlandite, biotite, and dolomite.

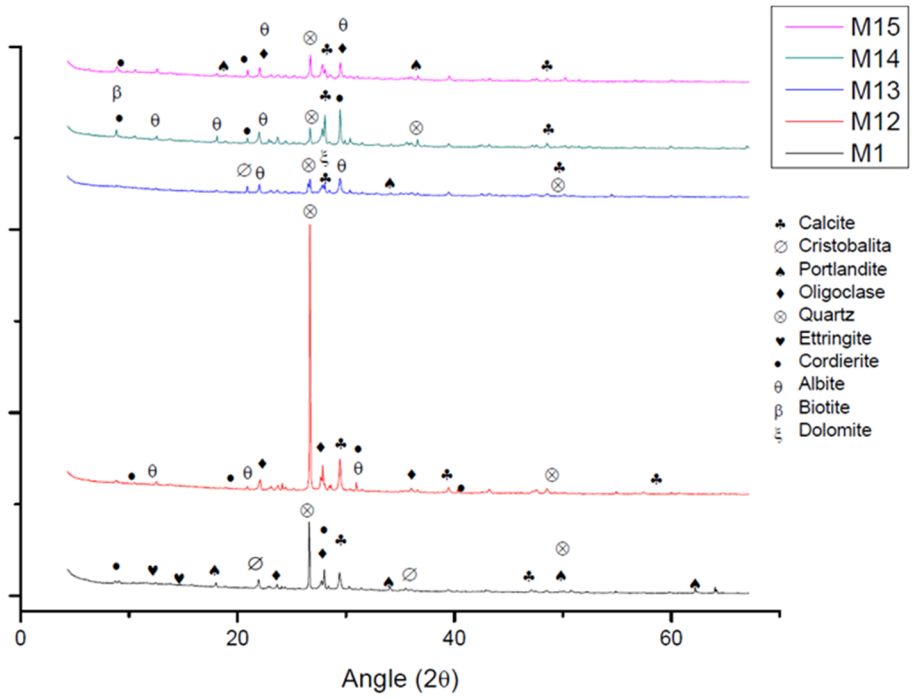

Figure 14. XRD after 270 days M1, M12, M13, M14, and M15.

Table 13. Quantification of composition found by XRD—metakaolin.

	Compound (%)												
Samples	**Calcite**	**Cristobalite**	**Quartz**	**Albite**	**Ettringite**	**Ferrosilite**	**Enstatite**	**Cordierite**	**Oligoclase**	**Portlandite**	**Chamosite**	**Anorthoclase**	**Total**
M1	9.1	4	46.5	-	3	-	-	12.2	23.2	2	-	-	100
M7	8	4	4	15	-	22	13	-	34	-	-	-	100
M8	11	5	8	27	-	-	-	-	42	-	7	-	100
M9	17	3	4	31	-	-	-	-	45	-	-	-	100
M10	10	2	4	-	-	-	-	-	70	-	-	13	100

Table 14. Quantification of composition found by XRD—foundry sand.

	Compound (%)										
Samples	**Calcite**	**Cristobalite**	**Quartz**	**Albite**	**Ettringite**	**Cordierite**	**Oligoclase**	**Portlandite**	**Biotite**	**Dolomite**	**Total**
M1	9.1	4	46.5	-	3	12.2	23.2	2	-	-	100
M12	8	-	39	14	-	21	18	-	-	-	100
M13	20	6	11	59	-	-	-	2	-	2	100
M14	14	9	9	11	-	25	-	-	32	-	100
M15	9	-	6	25	-	26	32	2	-	-	100

Figure 15a,b shows SEM results for the reference sample M1, which does not contain additives. Figure 15a shows the aggregate covered by hydrated cement paste, which is not homogeneous, showing some areas with more pores than others [59]. In Figure 15b, the characteristic ettringite structures can be seen, a phase that increases cohesion in cement and occurs at late ages [60]. The SEM results for the M2 sample, with 5% of the residual aggregate powder as addition, are presented in Figure 15c,d. Figure 15c shows the aggregate covered by hydrated cement paste [59]; the structure of ettringite can be seen in a pore [61]. Figure 15d shows the surface of the aggregate, surrounded by hydrated cement paste. The SEM results for the M3 sample, containing 10% of the residual aggregate powder, are shown in Figure 15e,f. Figure 16e shows hydrated cement paste [59], and within a pore, portlandite (calcium hydroxide), which acts as an "alkaline reserve", thus keeping the reinforced concrete protected against electrochemical corrosion [62]. Image 15f shows a portion of the aggregate surrounded by hydrated cement paste, as well as ettringite [61], on the surface. The SEM results for the M4 sample, containing 15% of the residual aggregate powder, are presented in Figure 15g,h. Figure 15g shows hydrated cement paste surrounding the aggregate, revealing some porosity in the paste. Figure 15h shows hydrated cement paste surrounding the aggregate, with ettringite surrounded by paste [61]. This hydrated cement phase increases the cohesion in the cement [62]. Figure 15i,j shows the SEM results for sample M5, containing 20% of the residual aggregate powder. Figure 15i shows hydrated cement paste surrounding the aggregate, covering it in a homogeneous way. The porosity in the paste can also be seen. Figure 15j is a higher magnification, where hydrated cement paste is seen surrounding the aggregate and C-S-H gel is presented [61], which is responsible for the adhesion of the paste with the aggregates [60]. Table 15 shows the elementary quantification found by EDS mapping, performed on each sample. It was found that all samples have C, O, Mg, Al, Si, Ca, and Fe, whereas Na, K, and Mn are found in some formulations.

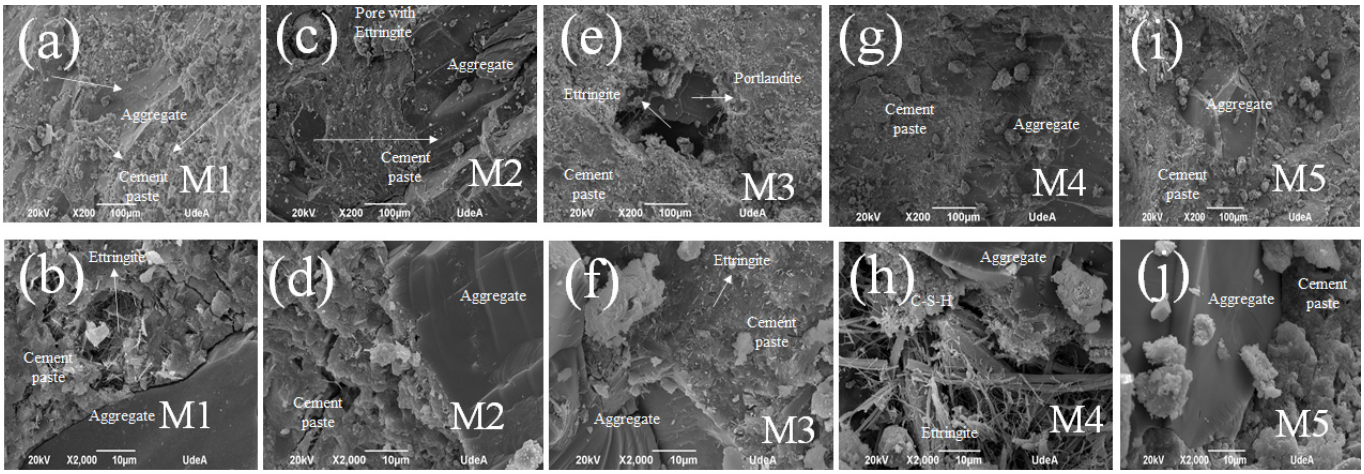

Figure 15. SEM of the five mixtures evaluated with residual aggregate powder.

Table 15. Elementary composition concrete with residual aggregate powder.

	Element (%)									
Samples	**C**	**O**	**Mg**	**Al**	**Si**	**Ca**	**Fe**	**Na**	**K**	**Mn**
M1	26.04	33.78	2.69	1.31	11.27	21.17	3.75	-	-	-
M2	20.31	28.26	0.38	6.70	18.41	22.58	1.17	2.19	-	-
M3	9.69	38.75	0.67	3.65	11.05	32.10	3.02	0.63	0.16	0.28
M4	17.36	31.22	0.60	4.18	16.34	25.71	2.78	0.99	0.83	-
M5	15.55	31.48	0.51	6.31	17.55	25.27	1.17	1.68	0.48	-

Figure 16a,b shows SEM images of the standard sample M1 just for comparison. Figure 16c,d shows SEM images for sample M7, which contains 5% of the metakaolin. Figure 16c shows hydrated cement paste surrounding the aggregate. Figure 16d shows the structure of the metakaolin in a portion that did not react. Figure 16e,f shows the SEM for sample M8, containing 10% of the metakaolin. Figure 16e shows hydrated cement paste surrounding the aggregate, whereas Figure 16f shows a higher magnification of the image, where hydrated cement paste is seen surrounding the aggregate. Figure 16g,h shows results for sample M9, containing 15% of metakaolin, where the hydrated cement paste is surrounding the aggregate. Figure 16h shows the image at a larger magnification, where hydrated cement paste is seen surrounding the aggregate and tobermorite gel or C-S-H [63]. Figure 16i,j shows results for sample M10, which contained 20% of the metakaolin as an addition. Figure 16i shows hydrated cement paste surrounding the aggregate. Figure 16j shows the image at a higher magnification, where hydrated cement paste is seen surrounding the aggregate and tobermorite gel (C-S-H) [61]. Table 16 shows the elementary quantification found by EDS mapping, performed on each sample. It was found that all samples have C, O, Mg, Al, Si, Ca, and Fe, whereas some samples do not have Na, K, and Ti.

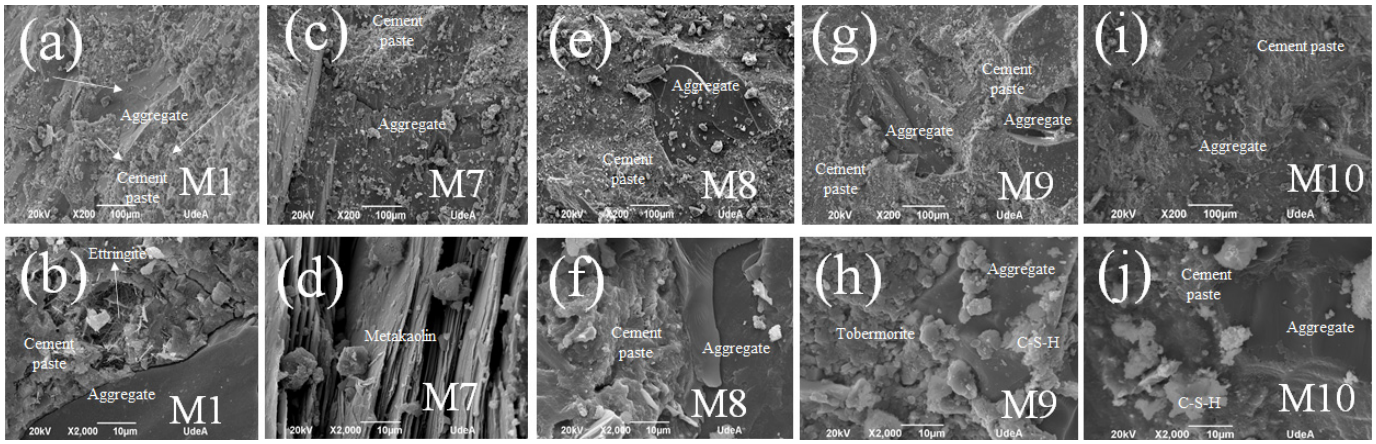

Figure 16. SEM of the five mixtures evaluated with metakaolin.

Table 16. Elementary composition concrete with metakaolin.

	Element (%)									
Samples	**C**	**O**	**Mg**	**Al**	**Si**	**Ca**	**Fe**	**Na**	**K**	**Ti**
M1	26.04	33.78	2.69	1.31	11.27	21.17	3.75	-	-	-
M7	14.67	28.68	-	14.25	28.58	9.92	0.81	2.09	1.00	-
M8	11.71	29.65	0.67	6.20	18.36	29.04	2.04	1.48	0.45	0.40
M9	14.62	42.71	0.21	4.76	12.10	22.88	0.63	1.77	0.32	-
M10	14.37	36.69	0.30	6.00	16.47	22.38	1.57	1.64	0.21	0.35

Figure 17a,b shows the results of the SEM test of the standard sample M1, just for comparison. Figure 17c,d shows results for sample M12, containing 5% of foundry sand. Figure 17c shows hydrated cement paste surrounding the aggregate. Figure 17d shows the hydrated cement paste surrounding the aggregate and tobermorite gel (C-S-H). Figure 17e,f shows sample M13, with 10% of the foundry sand, showing hydrated cement paste surrounding the aggregate. Ettringite is also observed. The results for sample M14, with 15% of the foundry sand, are presented in Figure 17g,h. Figure 17g shows hydrated cement paste surrounding the aggregate, with some hard to see porosity. Figure 17h shows the details of a pore, within which, ettringite, C-S-H gel (responsible for the adhesion of the paste with the aggregates), and portlandite (responsible for the protection of concrete against corrosion) are observed in this image. For sample M15, with 20% of foundry sand,

SEM images are shown in Figure 17i,j, revealing the cement paste surrounding the aggregate and tobermorite gel at two different magnifications. Table 17 shows the elementary quantification found by EDS mapping performed on each sample, where all samples have C, O, Mg, Al, Si, Ca, and Fe, whereas some samples do not have Na and K.

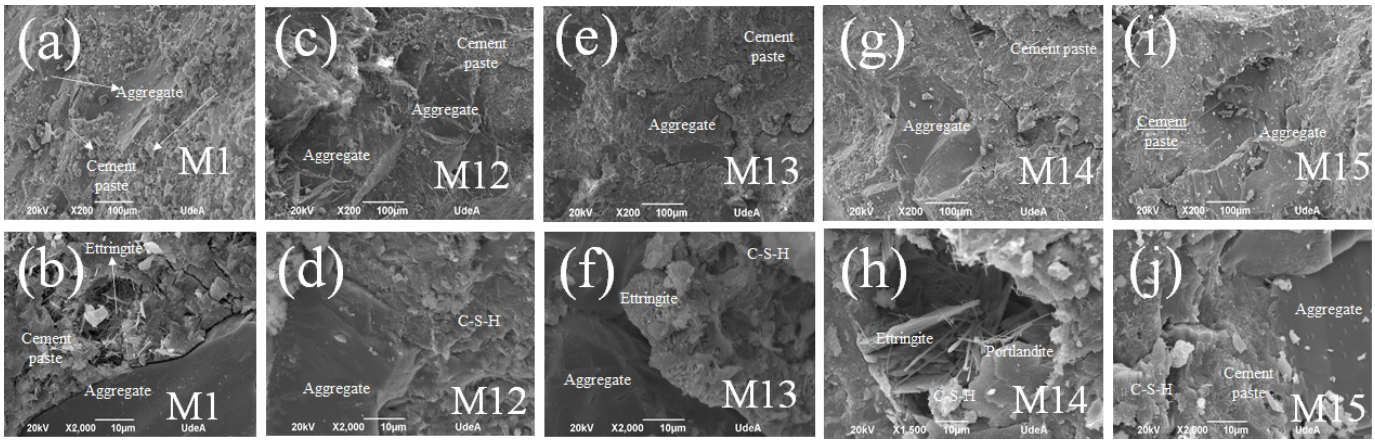

Figure 17. SEM of the five mixtures evaluated with foundry sand.

Table 17. Elementary composition concrete with foundry sand.

	Element (%)								
Samples	**C**	**O**	**Mg**	**Al**	**Si**	**Ca**	**Fe**	**Na**	**K**
M1	26.04	33.78	2.69	1.31	11.27	21.17	3.75	-	-
M12	12.37	29.72	1.3	6.43	33.23	9.91	2.83	1.85	2.65
M13	10.23	40.95	0.81	2.86	9.86	32.01	2.43	0.45	0.4
M14	16.86	29.22	0.73	2.07	10.02	37.85	3.24	-	-
M15	29.11	23.15	0.29	6.88	26.80	6.75	3.58	1.52	1.93

4. Discussion

The case study described in detail in this investigation is considered very successful for several reasons. First, there is a big part of the world where the implementation of some recycling technologies is not only not possible from an economic but also from a political point of view. Therefore, the combination of complex materials in relatively simple and accessible methods is a real solution, and its impact in terms of environmental and economic solutions can be large. This, in addition to a raw materials shortage in the concrete industry, is an important area where the current research shows high potential for providing solutions by combining solid wastes.

Recycled by-products from the ceramic industry, such as those used in this research, and particularly those from the metallurgical industry, are a worldwide problem. In addition, this research gives a real solution for two very different industries: steel smelting and quarry, both generating large amounts of solid waste. The complexity of these wastes forced companies from these sectors to dispose of them in landfills or in some cases illegally dispose of them in rivers. Both are not good solutions. In addition, this research is a company–university collaboration, which has proven to be a good example for large-scale implementations in the country, not only in the field but also for promoting and motivating politicians to generate new regulations that really enable the construction industry to use these novel materials. Moreover, from the materials engineering point of view, the use of these solid wastes reduced the amount of raw cement necessary in the concrete mix, as these by-products act as natural pozzolans replacing part of the cement, therefore helping decrease the CO_2 footprint.

Additionally, a comparison of concrete with a commercial metakaolin and two by-products, the residual aggregate powder and the foundry sand, showed the following

important results: the standard concrete resulted in a strength of 349 kgf/cm^2, corresponding to a 24% improvement with respect to the design strength of 280 kgf/cm^2 (27.5 MPa). Besides, concrete with the residual aggregate powder gave a strength of 541 kgf/cm^2 (53.1 MPa), which corresponds to M4 (concrete containing 15% of residual aggregate powder), corresponding to a 93% improvement with respect to the strength resistance. Furthermore, concrete with the foundry sand powder gave a strength of 561 kgf/cm^2 (55 MPa), corresponding to a 100% improvement with respect to the strength resistance, which corresponds to M15 (concrete containing 20% of foundry sand). Finally, concrete with the metakaolin powder presented a strength of 609 kgf/cm^2 (59.7 MPa), which corresponds to M9 (concrete containing 15% of metakaolin), corresponding to a 116% improvement with respect to the strength resistance.

These are very significant improvements that validate its use in infrastructure. This opens up research to the use of naturally occurring pozzolans, such as those with a volcanic origin, in great abundance in Central and South America [64]. The used by-products may have hydraulic and pozzolanic reactions. The first is chemical reactions in the presence of water that allows them to harden, like what happens with Portland cement. The second is the reactions of silica oxides in the presence of calcium hydroxides (portlandite) and water to form hydrated calcium silicates [65]. The calcium hydroxides that are one of the hydration products of Portland cement can also be produced by SCM itself by combining the CaO they contain with water [66]. The generation of hydrated calcium silicates from the pozzolanic reaction helps to densify the microstructure of the concrete, decrease its porosity, and increase its mechanical strength.

On the other hand, for a complete pozzolanic reaction and good curing in concrete, it is necessary to have an important amount of available water in the mix [67]. In this investigation, it was possible to maintain a good cure during the whole time of the test, since the cylinders were completely submerged, which contributed to a complete pozzolanic reaction of both the by-products and metakaolin.

The use of pozzolans as a complement to Portland cement generally influences reducing the heat of hydration because it has a lower percentage of the compounds responsible for raising the temperature during the setting of the cement, which implies a less capillary formation and therefore a greater density and compactness, which is reflected in a lower need for water to cure the elements made with this type of mixture. Furthermore, these additions improve the development of resistance and the durability of mortars and concrete [68]. The two by-products evaluated in this work are natural pozzolans (residual aggregate powder and foundry sand), and therefore gave appropriate results, far better than standard concrete, indicating that the concrete had greater compactness and density. The addition of MK to cement to generate mortars produces phase changes and microstructural transformations that affects the physical and chemical properties of the material. The OH- ions that are produced in the hydration of the cement are deposited in the pores of the concrete and when coming into contact with the amorphous silica of the pozzolans, as in the case of MK, an extra gel of hydrated calcium silicate is formed and the calcium hydroxide is reduced, giving important advantages to the mixtures, such as the increase in its mechanical strengths and the decrease in porosity, which is why it has been called a micro-filled effect. The MK reacts with the free calcium hydroxide [$Ca(OH)_2$] of the cement hydration process to form secondary C_2S, which subsequently forms the hydrated calcium silicate gel or tobermorite gel, the hydrated bicalcium silicoaluminate (gehlenite) and sometimes hydrogranates (hydrogarnet), which contribute to the improvement of the mechanical properties of the mixtures [69]. The metakaolin applicability has focused on artificial pozzolan in the production of mortars and concretes. Its pozzolanic activity, especially at an early age, is comparable to or superior to silica smoke and fly ash, which are two of the most widely used pozzolans in the world. In addition, it has the great advantage of its white color which allows its use in special applications and even in the production of added white cement [69]. In the samples analyzed with the XRD after 270 days (see Figures 12–14), the components were evidenced to have helped achieve high-strength con-

crete with acceptable amounts of cement, thus accomplishing concrete that is not expensive. This was revealed when the used by-products rose some of the compounds responsible for high strength, supported by SEM images. The solid waste materials used in this case study were residual aggregate powder and foundry sand, both classified as N-type ashes. On the other hand, Figures 6b, 8b and 10b were made based on the settlement (slump) of the concrete, tested just after the mixing and after 1 h of making the mixtures. With these graphs, it was shown that the concretes elaborated in this investigation must be used within an hour for any application; after this time, the concretes are not pumpable.

Figure 18 shows an economic analysis of the alternatives to concrete production. This graph shows the cost of each concrete formulation evaluated with the by-products and metakaolin. The cost of concrete with metakaolin is higher than with the by-products, which confirms the importance of using wastes and materials within reach. Concrete produced using the by-products would be more competitive at a commercial level since it could be cheaper and with similar characteristics to concrete with MK. Several eco-friendly solutions have been developed and implemented in Colombia as circular economy strategies in cementitious materials [70,71] and other building materials [72,73], aiming to reduce pollution by using concrete to hold solid wastes that are unproperly treated, reused, or disposed of. This research is a contribution to improve material circularity in the region and must be expanded for a larger impact on the environment.

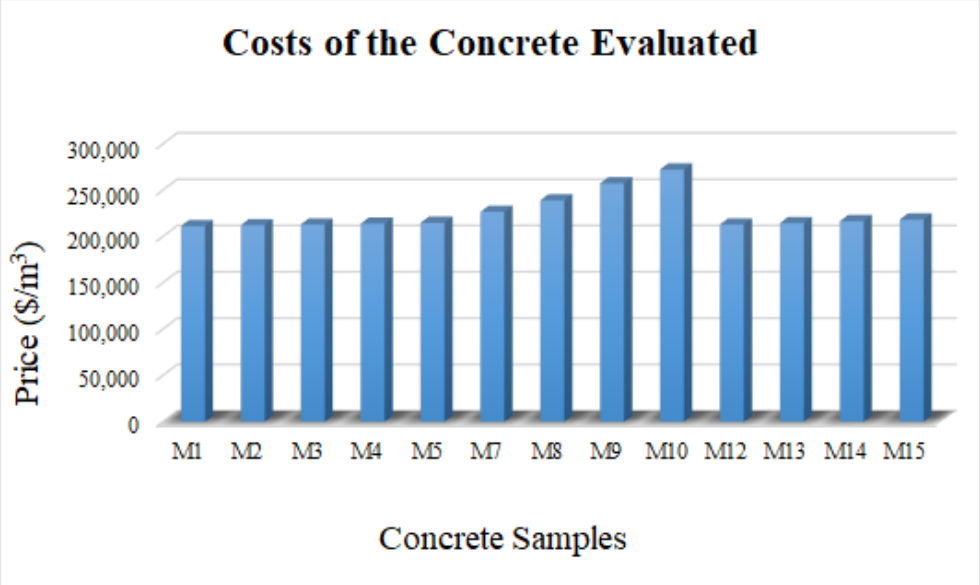

Figure 18. Costs of developed concrete.

In this study, the test of natural pozzolans was carried out for use as a mineral additive in Portland cement concrete, ASTM C311 standard, for the three materials studied. According to the standard, to be considered as materials with pozzolanic activity, these materials must have an index greater than 75% at 28 days. For the foundry sand, a 75.5% resistant activity index was obtained, meeting the standard requirements. According to the ASTM 311 standard, the fineness of these materials must be a minimum of 34% to be considered a pozzolan, and with the foundry sand, 65.4% was obtained. In relation to the addition of 20%, the concrete design was made based on 1 m^3 of concrete, and the additions were made based on the amount of cement. Thus, the additions increase the m^3 of designed concrete, with a good density of 2458 kg/m^3.

In this study, hydraulic concrete mixtures were designed as can be seen in Tables 5–7. These designs contained: cement, water, fine sand for concrete 3/8 of an inch (maximum size 9.53 mm), 3/4 inch gravel (maximum size 25.4 mm), plasticizer additive, and additions (foundry sand, residual aggregate powder-PB, or metakaolin). In Figure 1, we see the distribution of the particle sizes of the aggregates used, coarse (crushed 3/4 inch) and fine

(fine sand size 3/8 in), in order to provide the concrete with strength and give structure to it. In Figure 4, the morphology of the materials at a scale of 100 μm is evidenced, showing that the foundry sand and residual aggregate power do have a slightly larger particle size than cement and metakaolin, not to be used as fine aggregate, but as natural pozzolans. Although the specific surfaces of foundry sand and residual aggregate powder were not tested, with the measurement that was made of their fineness it can be seen that they are within the norm to be considered a natural pozzolan.

The presented results and method of this research can be fully applied to the particular mix of waste materials since they showed a strong influence on the properties of concrete. An important alteration in the waste chemistry may affect the microstructure and the corresponding properties; thus, results cannot be generalized to other wastes. This limitation is an opportunity to conduct more research depending on chemistry variation parameters which could include pH, calcium, other element variation contents, particle size distribution, and more.

5. Conclusions

- The industrial solid residues that were evaluated in this investigation—a residue from the steel foundry industry (foundry sand) and another from the aggregates industry (residual aggregate powder)—revealed that they had a pozzolanic activity index at 28 days for over 70%, showing that they can be used as additives in the production of hydraulic concrete and thus give them an environmentally sustainable use.
- The aggregates used in this study were obtained from an area in the center of the country. These showed that they had appropriate physical properties to produce hydraulic concrete, with a good aggregate size distribution. An important parameter was the wear in the Los Angeles machine, in which the aggregates presented percentages of wear of 23.9% (which is good considering that in Colombia a maximum wear of 40% is required). This gave an indication that the aggregate used had good mechanical characteristics.
- The by-products evaluated in this investigation as natural pozzolans (residual aggregate powder and foundry sand) can be classified as N-type pozzolans according to NTC 3493 since both by-products undergo calcination processes.
- The appearance of the hydraulic concrete made with the additions was in accordance with what was expected, since at the time of the production of concrete, it was sought that they were pasty, with good consistency and good initial fluidity, which is evidenced in the test of slump. This has been achieved with the addition of MK as a reference traditional material and with the two industrial residues.
- The by-products evaluated as natural pozzolans performed well in the evolution of the concrete strength. With the residual aggregate powder, an improvement of 93% in strength, 541 kgf/cm^2 (53.1 MPa), was obtained with respect to the design strength, 280 kgf/cm^2 (27.5 MPa), which corresponds to M4 (concrete containing 15% of residual aggregate powder). With foundry sand, an improvement of 100% in strength was achieved with respect to the design strength, 561 kgf/cm^2 (55 MPa), which corresponds to M15 (concrete containing 20% foundry sand). Concrete with the commercial metakaolin had a strength of 609 kgf/cm^2 (59.7 MPa), which is an improvement of 116% in strength, which corresponds to M9 (concrete containing 15% metakaolin), higher than by-products.
- The SEM and XRD were performed on the concrete cylinders after 270 days submerged in water and the samples did not show any unusual alteration in their components.
- As evidenced in the cost analysis that was carried out in this investigation, which was carried out with the prices that are handled in Colombia, the hydraulic concretes evaluated with by-products are economically more competitive than the hydraulic concretes with commercial MK. This is because MK is a commercial product and not a by-product.

Author Contributions: Conceptualization, H.A.C.; methodology, G.A., H.A.C.; validation, G.A., C.A.P. and H.A.C.; formal analysis, C.A.P. and S.N.M.; investigation, G.A.; resources, C.A.P. and H.A.C.; writing—original draft preparation, G.A., C.A.P., S.N.M. and H.A.C.; writing—review and editing, H.A.C. and S.N.M.; project administration, H.A.C.; funding acquisition, H.A.C. and C.A.P. All authors have read and agreed to the published version of the manuscript.

Funding: This research was partially supported by Universidad de Antioquia and Conasfaltos SAS.

Institutional Review Board Statement: Not applicable.

Informed Consent Statement: Not applicable.

Data Availability Statement: Not applicable.

Acknowledgments: Authors want to thank to Conasfaltos S.A. collaboration during this research.

Conflicts of Interest: The authors declare no conflict of interest.

References

1. Conner, J.R.; Hoeffner, S.L. A Critical Review of Stabilization/Solidification Technology. *Crit. Rev. Environ. Sci. Technol.* **2010**, *28*, 397–462. [CrossRef]
2. Agudelo, G.; Cifuentes, S.; Colorado, H.A. Ground Tire Rubber and Bitumen with Wax and Its Application in a Real Highway. *J. Clean. Prod.* **2019**, *228*, 1048–1061. [CrossRef]
3. El-Eswed, B.I.; Aldagag, O.M.; Khalili, F.I. Efficiency and Mechanism of Stabilization/Solidification of Pb(II), Cd(II), Cu(II), Th(IV) and U(VI) in Metakaolin Based Geopolymers. *Appl. Clay Sci.* **2017**, *140*, 148–156. [CrossRef]
4. Colorado, H.A.; Singh, D. High-Sodium Waste Streams Stabilized with Inorganic Acid–Base Phosphate Ceramics Fabricated at Room Temperature. *Ceram. Int.* **2014**, *40*, 10621–10631. [CrossRef]
5. Dahale, P.D.; Nagarnaik, P.B.; Gajbhiye, A.R. Utilization of Solid Waste for Soil Stabilization: A Review. *Electron. J. Geotech. Eng.* **2012**, *17*, 2443–2461.
6. Naik, T.R.; Moriconi, G. Environmental Friendly Durable Concrete Made with Recycled Materials for Sustainable Concrete Construction. *Proc. Int. Symp. Sustain. Dev. Cem.* **2005**, *5*, 485–505. [CrossRef]
7. Czarnecki, L.; Justnes, H. Sustainable and Durable Concrete. *Cement-Wapno-Beton* **2012**, *17*, 341.
8. Ghafourian, K.; Kabirifar, K.; Mahdiyar, A.; Yazdani, M.; Ismail, S.; Tam, V.W.Y. A Synthesis of Express Analytic Hierarchy Process (EAHP) and Partial Least Squares-Structural Equations Modeling (PLS-SEM) for Sustainable Construction and Demolition Waste Management Assessment: The Case of Malaysia. *Recycling* **2021**, *6*, 73. [CrossRef]
9. Avet, F.; Li, X.; Scrivener, K. Determination of the Amount of Reacted Metakaolin in Calcined Clay Blends. *Cem. Concr. Res.* **2018**, *106*, 40–48. [CrossRef]
10. Aiswarya, S.; Prince Arulraj, G.; Dilip, C. A Review on Use of Metakaolin in Concrete. *Eng. Sci. Technol. Int. J.* **2013**, *3*, 592–597.
11. Nova, J. Strength Properties of Metakaolin Admixed Concrete. *Int. J. Sci. Res. Publ.* **2013**, *3*, 1–7.
12. Chandak, M.A.; Pawade, P.Y. Influence of Metakaolin in Concrete Mixture: A Review. *IJES* **2018**, *1*, 37–41.
13. Thomas, M. The Effect of Supplementary Cementing Materials on Alkali-Silica Reaction: A Review. *Cem. Concr. Res.* **2011**, *41*, 1224–1231. [CrossRef]
14. Yen, T.; Hsu, T.H.; Liu, Y.W.; Chen, S.H. Influence of Class F Fly Ash on the Abrasion–Erosion Resistance of High-Strength Concrete. *Constr. Build. Mater.* **2007**, *21*, 458–463. [CrossRef]
15. Rodríguez-Camacho, R.E.; Uribe-Afif, R. Importance of Using the Natural Pozzolans on Concrete Durability. *Cem. Concr. Res.* **2002**, *32*, 1851–1858. [CrossRef]
16. Thomas, M. Optimizing the Use of Fly Ash in Concrete. *Portland Cem. Assoc.* **2007**, *5420*, 24.
17. Shahmansouri, A.A.; Yazdani, M.; Ghanbari, S.; Akbarzadeh Bengar, H.; Jafari, A.; Farrokh Ghatte, H. Artificial Neural Network Model to Predict the Compressive Strength of Eco-Friendly Geopolymer Concrete Incorporating Silica Fume and Natural Zeolite. *J. Clean. Prod.* **2021**, *279*, 123697. [CrossRef]
18. Omrane, M.; Kenai, S.; Kadri, E.H.; Aït-Mokhtar, A. Performance and Durability of Self Compacting Concrete Using Recycled Concrete Aggregates and Natural Pozzolan. *J. Clean. Prod.* **2017**, *165*, 415–430. [CrossRef]
19. Zerbino, R.; Giaccio, G.; Batic, O.R.; Isaia, G.C. Alkali–Silica Reaction in Mortars and Concretes Incorporating Natural Rice Husk Ash. *Constr. Build. Mater.* **2012**, *36*, 796–806. [CrossRef]
20. Fapohunda, C.; Akinbile, B.; Shittu, A. Structure and Properties of Mortar and Concrete with Rice Husk Ash as Partial Replacement of Ordinary Portland Cement—A Review. *Int. J. Sustain. Built Environ.* **2017**, *6*, 675–692. [CrossRef]
21. Ling, T.C.; Poon, C.S. Spent Fluorescent Lamp Glass as a Substitute for Fine Aggregate in Cement Mortar. *J. Clean. Prod.* **2017**, *161*, 646–654. [CrossRef]
22. Kazmi, S.M.S.; Munir, M.J.; Patnaikuni, I.; Wu, Y.F. Pozzolanic Reaction of Sugarcane Bagasse Ash and Its Role in Controlling Alkali Silica Reaction. *Constr. Build. Mater.* **2017**, *148*, 231–240. [CrossRef]
23. Icontec. *NTC 3493. Fly Ash and Raw or Calcined Natural Pozzolan for Use in Concrete*; Icontec: Bogotá, Colombia, 2019; p. 11.
24. Foundry Industry Recycling Starts Today (FIRST). *Foundry Sand Facts for Civil Engineers*; FIRST: Fall River, MA, USA, 2004.

25. Ricardo, A.R. *La Arena Residual de Fundición y Su Revalorización Para La Industria de Construcción*; Universidad Autonoma del Estado de Hidalgo: Sahagún, Mexico, 2012.
26. Iqbal, M.F.; Javed, M.F.; Rauf, M.; Azim, I.; Ashraf, M.; Yang, J.; Liu, Q.; Iqbal, M.F.; Javed, M.F.; Rauf, M.; et al. Sustainable Utilization of Foundry Waste: Forecasting Mechanical Properties of Foundry Sand Based Concrete Using Multi-Expression Programming. *ScTEn* **2021**, *780*, 146524. [CrossRef] [PubMed]
27. Guney, Y.; Sari, Y.D.; Yalcin, M.; Tuncan, A.; Donmez, S. Re-Usage of Waste Foundry Sand in High-Strength Concrete. *Waste Manag.* **2010**, *30*, 1705–1713. [CrossRef] [PubMed]
28. Explotación de Materiales de Construcción: Canteras y Material de Arrastre. Available online: https://repositoriobi.minenergia.gov.co/handle/123456789/2445 (accessed on 23 May 2022).
29. Forde, M. Fundamentals and Theory, Concrete, Asphalts in Road Construction. In *ICE Manual of Construction Materials: Fundamentals and Theory, Concrete, Asphalts in Road Construction, Masonry*; ICE: London, UK, 2009; Volume 1.
30. Statista Cement: Production Ranking Top Countries 2021 | Statista. Available online: https://www.statista.com/statistics/267364/world-cement-production-by-country/ (accessed on 24 May 2022).
31. Rubenstone, J. PCA Forecasts Growth in Cement Consumption at World of Concrete 2016 | 2016-02-02 | ENR | Engineering News-Record. Available online: https://www.enr.com/articles/38747-pca-forecasts-growth-in-cement-consumption-at-world-of-concrete-2016 (accessed on 27 June 2022).
32. DANE Estadísticas de Concreto Premezclado. Available online: https://www.dane.gov.co/index.php/estadisticas-por-tema/construccion/estadisticas-de-concreto-premezclado (accessed on 23 May 2022).
33. Zapata, J.F.; Azevedo, A.; Fontes, C.; Monteiro, S.N.; Colorado, H.A. Environmental Impact and Sustainability of Calcium Aluminate Cements. *Sustainability* **2022**, *14*, 2751. [CrossRef]
34. Colorado, H.A.; Muñoz, A.; Neves Monteiro, S. Circular Economy of Construction and Demolition Waste: A Case Study of Colombia. *Sustainability* **2022**, *14*, 7225. [CrossRef]
35. Castañeda, M.; Gutiérrez-Velásquez, E.I.; Aguilar, C.E.; Monteiro, S.N.; Amell, A.A.; Colorado, H.A. Sustainability and Circular Economy Perspectives of Materials for Thermoelectric Modules. *Sustainability* **2022**, *14*, 5987. [CrossRef]
36. Colorado, H.A.; Gutiérrez-Velásquez, E.I.; Monteiro, S.N. Sustainability of Additive Manufacturing: The Circular Economy of Materials and Environmental Perspectives. *J. Mater. Res. Technol.* **2020**, *9*, 8221–8234. [CrossRef]
37. Ordoñez, E.; Neves Monteiro, S.; Colorado, H.A. Valorization of a Hazardous Waste with 3D-Printing: Combination of Kaolin Clay and Electric Arc Furnace Dust from the Steel Making Industry. *Mater. Des.* **2022**, *217*, 110617. [CrossRef]
38. Vergara, L.A.; Colorado, H.A. Additive Manufacturing of Portland Cement Pastes with Additions of Kaolin, Superplastificant and Calcium Carbonate. *Constr. Build. Mater.* **2020**, *248*, 118669. [CrossRef]
39. Icontec. *NTC 174. Specification for Concrete Aggregates*; Icontec: Bogotá, Colombia, 2018; p. 30.
40. Icontec. *NTC 92. Test Method for the Determination of Bulk Density ("Unit Weight") and Voids in Aggregate*; Icontec: Bogotá, Colombia, 2019; p. 13.
41. INVIAS. *INV E-222. Specific Gravity and Absorption of Fine Aggregates*; INVIAS: Bogotá, Colombia, 2013; p. 17.
42. INVIAS. *INV E 500. Hydraulic Concrete Pavement*; INVIAS: Bogotá, Colombia, 2013; p. 74.
43. Icontec. *NTC 33. Test Method to Determine the Fineness of Hydraulic Cement by the Blaine Air-Permeability Apparatus*; Icontec: Bogotá, Colombia, 2019; p. 22.
44. Icontec. *NTC 294. Test Method to Determine the Fineness of Hydraulic Cement by the 45 Mm (No. 325) Sieve*; Icontec: Bogotá, Colombia, 2018.
45. Icontec. *NTC 107. Test Method for Autoclave Expansion of Hydraulic Cement*; Icontec: Bogotá, Colombia, 2019; p. 9.
46. Icontec. *NTC 118. Test Method for Determining the Time of Setting of Hydraulic Cement by Vicat Needle*; Icontec: Bogotá, Colombia, 2020.
47. Icontec. *NTC 224. Test Method to Determine the Air Content of Hydraulic Cement Mortar*; Icontec: Bogotá, Colombia, 2020; p. 12.
48. Icontec. *NTC 220. Determination of Compressive Strength of Hydraulic Cement Mortars, Using 50 Mm or 2 Inches Cube Specimens*; Icontec: Bogotá, Colombia, 2021; p. 25.
49. Icontec. *NTC 4927. Test Method for Determining the Test Method to Measure Expansion of Hydraulic Cement Mortar Bars Stored in Water*; Icontec: Bogotá, Colombia, 2020; p. 8.
50. ASTM. *ASTM C618. Standard Specification for Coal Fly Ash and Raw or Calcined Natural Pozzolan for Use in Concrete*; ASTM: West Conshohocken, PA, USA, 2019.
51. ASTM. *ASTM C494. Standard Specification for Chemical Admixtures for Concrete*; ASTM: West Conshohocken, PA, USA, 2019.
52. Diaz, V. *Método Para El Diseño de Hormigón de Alto Comportamiento*; Univeridad del Valle: Cali, Colombia, 1997; ISBN 9586701263.
53. Restrepo Gutiérrez, J.C.; Restrepo Baena, O.J.; Tubón, J.I. Efectos de La Adición de Metacaolín En El Cemento Pórtland. *DYNA* **2006**, *73*, 131–141.
54. Penkaitis, G.; Sígolo, J.B. Waste Foundry Sand. Environmental Implication and Characterization. *Geol. USP Ser. Cient.* **2012**, *12*, 57–70. [CrossRef]
55. Gill, A.S.; Siddique, R. Durability Properties of Self-Compacting Concrete Incorporating Metakaolin and Rice Husk Ash. *Constr. Build. Mater.* **2018**, *176*, 323–332. [CrossRef]
56. Icontec. *NTC 396. Test Method to Determine the Slump of the Concrete*; Icontec: Bogotá, Colombia, 2021; p. 11.
57. Icontec. *NTC 673. Test Method for Compressive Strength of Cylindrical Concrete Specimens*; Icontec: Bogotá, Colombia, 2021; p. 21.
58. Kareem, T.A.; Kaliani, A.A. Glow Discharge Plasma Electrolysis for Nanoparticles Synthesis. *Ionics* **2011**, *18*, 315–327. [CrossRef]

59. Mouret, M.; Bascoul, A.; Escadeillas, G. Microstructural Features of Concrete in Relation to Initial Temperature—SEM and ESEM Characterization. *Cem. Concr. Res.* **1999**, *29*, 369–375. [CrossRef]
60. Metha, P.K.; Monteiro, P.J.M. *Concrete: Microstructure, Properties, and Materials (Mechanical Engineering)*; McGraw-Hill Education: New York, NY, USA, 2013; ISBN 978-0071797870.
61. Demir, I.; Guzelkucuk, S.; Sevim, O.; Filazi, A.; Sengul, C.G. Examination of Microstructure of Fly Ash in Cement Mortar. *Int. J. Adv. Mech. Civ. Eng.* **2018**, 2394–2827.
62. Gerardo, G. *Concreto Simple*; Universidad del Cauca: Popayán, Colombia, 2013.
63. Shen, P.; Lu, L.; Chen, W.; Wang, F.; Hu, S. Efficiency of Metakaolin in Steam Cured High Strength Concrete. *Constr. Build. Mater.* **2017**, *152*, 357–366. [CrossRef]
64. Adesina, P.A.; Olutoge, F.A. Structural Properties of Sustainable Concrete Developed Using Rice Husk Ash and Hydrated Lime. *J. Build. Eng.* **2019**, *25*, 100804. [CrossRef]
65. Paris, J.M.; Roessler, J.G.; Ferraro, C.C.; Deford, H.D.; Townsend, T.G. A Review of Waste Products Utilized as Supplements to Portland Cement in Concrete. *J. Clean. Prod.* **2016**, *121*, 1–18. [CrossRef]
66. Hewlett, P.C.; Liska, M. Lea's Chemistry of Cement and Concrete. *Lea's Chem. Cem. Concr.* **2019**, *5*, 1–858. [CrossRef]
67. Papadakis, V.G.; Antiohos, S.; Tsimas, S. Supplementary Cementing Materials in Concrete: Part II: A Fundamental Estimation of the Efficiency Factor. *Cem. Concr. Res.* **2002**, *32*, 1533–1538. [CrossRef]
68. Thomas, M. *Supplementary Cementing Materials in Concrete*; CRC Press: Boca Raton, FL, USA, 2013; ISBN 1466572981.
69. Rakhimova, N.R.; Rakhimov, R.Z. Reaction Products, Structure and Properties of Alkali-Activated Metakaolin Cements Incorporated with Supplementary Materials—A Review. *J. Mater. Res. Technol.* **2019**, *8*, 1522–1531. [CrossRef]
70. Colorado, H.A.; Wang, Z.; Yang, J.M. Inorganic Phosphate Cement Fabricated with Wollastonite, Barium Titanate, and Phosphoric Acid. *Cem. Concr. Compos.* **2015**, *62*, 13–21. [CrossRef]
71. Florez, R.; Colorado, H.A.; Alajo, A.; Giraldo, C.H.C. The Material Characterization and Gamma Attenuation Properties of Portland Cement-Fe_3O_4 Composites for Potential Dry Cask Applications. *Prog. Nucl. Energy* **2019**, *111*, 65–73. [CrossRef]
72. Loaiza, A.; Cifuentes, S.; Colorado, H.A. Asphalt Modified with Superfine Electric Arc Furnace Steel Dust (EAF Dust) with High Zinc Oxide Content. *Constr. Build. Mater.* **2017**, *145*, 538–547. [CrossRef]
73. Revelo, C.F.; Correa, M.; Aguilar, C.; Colorado, H.A. Composite Materials Made of Waste Tires and Polyurethane Resin: A Case Study of Flexible Tiles Successfully Applied in Industry. *Case Stud. Constr. Mater.* **2021**, *15*, e00681. [CrossRef]